

Article

Spatial Rearrangement and Mobility Heterogeneity of an Anionic Lipid Monolayer Induced by the Anchoring of Cationic Semiflexible Polymer Chains

Xiaozheng Duan ¹, Yang Zhang ², Ran Zhang ¹, Mingming Ding ^{1,*}, Tongfei Shi ^{1,*}, Lijia An ¹, Qingrong Huang ³ and Wen-Sheng Xu ^{4,*}

¹ State Key Laboratory of Polymer Physics and Chemistry, Changchun Institute of Applied Chemistry, Chinese Academy of Sciences, Changchun 130022, China; xzduan@ciac.ac.cn (X.D.); rzhangciac@ciac.ac.cn (R.Z.); lljan@ciac.ac.cn (L.A.)

² School of Business, Northeast Normal University, Changchun 130024, China; yzhang_nenu@hotmail.com

³ Department of Food Science, Rutgers University, 65 Dudley Road, New Brunswick, NJ 08901, USA; qhuang@aesop.rutgers.edu

⁴ James Franck Institute, The University of Chicago, Chicago, IL 60637, USA

* Correspondence: mmding@ciac.ac.cn (M.D.); tfshi@ciac.ac.cn (T.S.); wsxu@uchicago.edu (W.-S.X.); Tel.: +86-431-8526-2516 (M.D.); +86-431-8526-2309 (T.S.); +1-773-366-0112 (W.-S.X.)

Academic Editor: Martin Kröger

Received: 12 May 2016; Accepted: 13 June 2016; Published: 17 June 2016

Abstract: We use Monte Carlo simulations to investigate the interactions between cationic semiflexible polymer chains and a model fluid lipid monolayer composed of charge-neutral phosphatidyl-choline (PC), tetravalent anionic phosphatidylinositol 4,5-bisphosphate (PIP₂), and univalent anionic phosphatidylserine (PS) lipids. In particular, we explore how chain rigidity and polymer concentration influence the spatial rearrangement and mobility heterogeneity of the monolayer under the conditions where the cationic polymers anchor on the monolayer. We find that the anchored cationic polymers only sequester the tetravalent PIP₂ lipids at low polymer concentrations, where the interaction strength between the polymers and the monolayer exhibits a non-monotonic dependence on the degree of chain rigidity. Specifically, maximal anchoring occurs at low polymer concentrations, when the polymer chains have an intermediate degree of rigidity, for which the PIP₂ clustering becomes most enhanced and the mobility of the polymer/PIP₂ complexes becomes most reduced. On the other hand, at sufficiently high polymer concentrations, the anchoring strength decreases monotonically as the chains stiffen—a result that arises from the pronounced competitions among polymer chains. In this case, the flexible polymers can confine all PIP₂ lipids and further sequester the univalent PS lipids, whereas the stiffer polymers tend to partially dissociate from the monolayer and only sequester smaller PIP₂ clusters with greater mobilities. We further illustrate that the mobility gradient of the single PIP₂ lipids in the sequestered clusters is sensitively modulated by the cooperative effects between anchored segments of the polymers with different rigidities. Our work thus demonstrates that the rigidity and concentration of anchored polymers are both important parameters for tuning the regulation of anionic lipids.

Keywords: semiflexible polymers; anchoring; sequestration; mobility; anionic lipid; Monte Carlo

1. Introduction

A deep understanding of the interactions between peripheral cationic bio-macromolecules and anionic lipid membranes is crucial for many cellular activities [1,2], including ion-channel activation, vesicle trafficking, cellular apoptosis, enzyme activation, *etc.* The key component in the lipid membrane that launches the anchoring of bio-macromolecules is the phosphatidylinositol 4,5-bisphosphate (PIP₂)

lipid, which has a valence of -4 at $\text{pH} = 7.0$ [3], and therefore enables the electrostatic anchoring of proteins or polypeptides with a cluster of polybasic residues. Despite the fact that PIP_2 lipids constitute only about 1% of all phospholipids in the plasma membrane, this versatile lipid species is essential for nearly all signaling functions in living cells [1,4,5]. As another important functional phospholipid, phosphatidylserine (PS) has a single net negative charge and constitutes about 10%–20% of all lipids. The univalent PS lipids can thus regulate the surface charge density of the membrane to induce the anchoring of cationic polymers, thereby controlling some specific physiological activities [2,6].

The complex coacervates of charged macromolecules and liposomes have been extensively studied via a variety of experimental techniques [1,4,6–10], such as X-ray scattering, transmission electron microscopy, fluorescence resonance energy transfer measurements, *etc.* These studies have demonstrated that the anchored charged macromolecules can adjust the fraction of free anionic lipids and cause the mobility heterogeneity of the membrane through the electrostatic sequestration of the anionic lipids, thereby offering useful information for the development of biological and medical applications [11–16]. However, it remains a significant challenge to investigate the macromolecule/membrane complexes at a molecular scale via experimental approaches, due to the hydrolysis and fast turnover of the anionic lipids *in vivo* [1]. In particular, it is generally difficult to investigate the influence of each individual molecular parameter on the interactions between charged macromolecules and liposomes experimentally. Hence, computational and theoretical methods provide complementary tools for better understanding the mechanisms of these interfacial interactions. For example, a recent study based on the atomic model [17] indicates that the anchored polypeptides can cause the sequestration and dynamic restriction of anionic lipids, which theoretically rationalizes the experimental measurements via microscopy. The coarse-grained models have also been widely employed in simulations to elucidate the biophysical properties of the macromolecule/membrane complex coacervates [18–28]. Results from these models have demonstrated that several important molecular factors—such as the shape, size, and ionization degree of the peripheral macromolecules, and the charge of the lipids—all affect the stability, structure, and dynamics of the complexes significantly. While the intrinsic rigidity evidently represents an important characteristic feature of the peripheral cationic macromolecules, the influence of this important molecular parameter on the structure and dynamics of membrane/macromolecule complexes has been addressed in a limited way in previous simulations [1,22]. Moreover, the concentration of peripheral macromolecules often varies considerably from one region to another *in vivo*; e.g., the growth-associated protein 43 exhibits a higher concentration in the axonal growth cones of neurons and some other regions [1,29]. Therefore, it is then natural to ask how the rigidity and concentration of polymers determine their anchoring on lipid membranes, and how these factors affect the resulting properties of macromolecule/membrane complexes.

Our recent work based on Monte Carlo (MC) simulations has investigated the anchoring of a single flexible cationic polymer onto a fluid monolayer composed of charge-neutral and anionic lipids [30–32]. Our simulations show that the cationic polymer can cause significant sequestration of the anionic lipids and reduce mobility of the lipids. Our work also indicates that the sequestration and mobility of the anionic lipids are strongly dependent on the charge of lipid headgroups and the ionic strength of the solution. These trends are in qualitative agreement with recent experimental studies [7]. Our previous work also addresses the effects of chain rigidity on the stability and corresponding entropy–energy balance of the polymer/monolayer complex [33,34], where only a single polymer chain anchored on the lipid membrane is considered. In this paper, we further extend our study to the anchoring of multiple cationic polymers with variable chain stiffness onto a fluid mixed lipid monolayer, and therefore, we explicitly explore how chain rigidity and polymer concentration affect the properties of macromolecule/membrane complexes with a particular focus on the sequestration and mobility heterogeneity of the anionic lipids.

The rest of the paper is organized as follows. In Section 2, we introduce the MC model and provide a brief introduction to the simulation details. In Section 3, we discuss the interactions between the anchored polymers and the monolayer and analyze the effects of polymer rigidity and concentration

on the structure and mobility of the polymers/monolayer complex. In Section 4, we draw some concluding remarks.

2. Model and Simulation Method

2.1. Monte Carlo Model

Our Monte Carlo (MC) model of the polymers/monolayer complex has been described in detail in our previous work [30–34], so we briefly introduce this model here. We employ the freely-jointed chain model to coarse-grain the cationic polymers [35]. Each polymer chain includes $N = 20$ connected segments, with each segment taking a positive charge of $Z_s = +1$ at its center. All segments have the same diameter of $d = 8.66 \text{ \AA}$. The lipid monolayer is composed of 50×50 lipid headgroups, which are modeled as 2500 hexagonal closely-packed disks (also with a diameter of $d = 8.66 \text{ \AA}$) on an impenetrable plane at $z = 0$ of the simulation box. The monolayer contains the charge-neutral phosphatidyl-choline (PC), the univalent PS, and the tetravalent PIP₂ lipid molecules. Driven by the biophysical interests [1,22], we consider the following compositions of the monolayer in this work: PC:PS:PIP₂ = 98:1:1, PC:PIP₂ = 99:1 and PC:PS:PIP₂ = 89:10:1. While the composition with PC:PIP₂ = 99:1 permits investigations of the interactions between anchored polymers and the anionic tetravalent PIP₂ lipids, we can further compare the sequestration and mobility heterogeneity of both PS and PIP₂ lipids caused by polymer anchoring for PC:PS:PIP₂ = 98:1:1. The case with PC:PS:PIP₂ = 89:10:1 represents the membrane with more realistic lipid compositions, as discussed in Refs. [22,24]. However, since the general trends of the examined properties are quite similar for different compositions, we mainly focus on the case of PC:PS:PIP₂ = 98:1:1 and briefly discuss the results for the other compositions.

We express the potential energy of the system in the form of

$$U = U_{\text{NB}} + U_{\text{bend}} \quad (1)$$

where U_{NB} and U_{bend} designate the contributions arising from non-bonded and angular interactions, respectively. Since we fix the bond length of the polymers as a constant of d , the contribution from bonded interactions to the potential energy is simply zero. The non-bonded contribution U_{NB} contains the hard sphere potential (U_{HS}) between polymer segments and the electrostatic potential (U_{E}) between charged species,

$$U_{\text{NB}} = U_{\text{HS}} + U_{\text{E}} \quad (2)$$

We consider the polymers/monolayer complex in a symmetric univalent salt aqueous solution, and further account for the electrostatic interactions between charged species through Debye–Hückel theory,

$$U_{\text{E}} = \frac{1}{2} k_{\text{B}} T \sum_{m \neq n} Z_m Z_n l_{\text{B}} \frac{\exp(-l_{\text{D}} r_{\text{mn}})}{r_{\text{mn}}} \quad (3)$$

where Z_m and Z_n are the valences of the charges m and n , r_{mn} is the distance between charges m and n , l_{B} is the Bjerrum length taken as 7.14 \AA in aqueous solution at 278 K, and l_{D} is the inverse Debye screening length. We adopt the Debye screening length (l_{D}^-) to account for the screen effects from the solution,

$$l_{\text{D}}^- = \frac{1}{\sqrt{1000 e^2 N_{\text{A}} \sum_i \frac{Z_i^2 C_i}{\varepsilon_0 \varepsilon_r k_{\text{B}} T}}} \quad (4)$$

where e is the elementary charge, N_{A} is Avogadro's constant, Z_i is the valence of the salt ions, C_i is the salt concentration of the solution, and ε_r is the dielectric permittivity, which equals ~ 78.5 in the salt solution and ~ 2 within the monolayer [23,24]. The energy and distance are expressed in units of $k_{\text{B}} T$ and d , respectively.

We further adopt a harmonic bending potential U_{bend} to adjust the intrinsic rigidity of the cationic polymers,

$$U_{\text{bend}} = \kappa k_B T \sum_{i=2}^{N-1} (\alpha_i - \alpha_0)^2 \quad (5)$$

where α_i denotes the angle specified by the connected segments $i + 1$, i , and $i - 1$, α_0 equals π , and the chain rigidity parameter κ tailors the strength of angular interactions and hence the degree of chain rigidity. It is then expected that elevating κ leads to an increase in the persistence length (L_p), which we analyze below by computing this quantity from the bond angle correlation function in our simulations. While our model is clearly rather idealized, we expect that it can capture some qualitative trends that will be useful for better understanding the interactions between bio-macromolecules and lipid membranes.

2.2. Simulation Details

We perform simulations in an NVT ensemble. Periodical boundary conditions are applied in the x and y directions, and the z direction is taken as infinite. We implement the relaxation of the polymers via kink-jump, crankshaft, translation and pivot movements [36], and employ the Kawasaki algorithm [25,37,38] to model the lipid motions. Each MC step includes the trial movements of all polymer segments and charged lipids in accordance with the Metropolis algorithm [39]. In each run, we put the cationic polymers onto the monolayer and generate the anionic lipids on the monolayer stochastically. We first perform 10^6 MC steps for athermal relaxation in order to eliminate the artificial effects from the initial configuration, and the polymers are controlled to relax above the monolayer at this stage. We then perform 2×10^6 MC steps for equilibration, and another 2×10^6 MC steps for data analysis. For each state point, we run 20 parallel simulations.

We vary the rigidity parameter κ of the polymers from 0 to 100, a range of values that allows for the simulation of fully flexible chains ($\kappa = 0$), chains with intermediate rigidity ($0 < \kappa \leq 20$), and chains with high rigidity ($\kappa > 20$). The effect of polymer concentration is explored by adjusting the number N_c of polymer chains from 2, 4, 8, to 16. These chain numbers can be converted into polymer concentrations ($C_p = N_c/A_m$) as 0.00092, 0.00185, 0.0037, to 0.0074 [d^{-2}], where the concentration is measured via the number of chains per unit area. Since our interest here is to study the polymers/monolayer interactions, we mainly consider the cases with the salt concentration of $C_i = 0.01$ M, for which the polymers anchor onto the monolayer. We only briefly discuss the salt effect of the solution on the stability and mobility of the complex.

To characterize the stiffness of the polymer chains, we calculate the bond angle correlation function $BAC(D_C) \sim e^{(-D_C/L_p)}$ [40] to extract the persistence length L_p of the cationic polymers, where D_C denotes the contour distance along the polymer chain and L_p includes the electrostatic contribution (L_e) and the intrinsic part (L_0). In Table 1, we summarize the persistence length L_p of the polymers for various κ at different salt concentrations C_i . We see that L_p increases with κ for fixed C_i , as expected. Moreover, the salt concentration C_i exerts a strong impact on L_p .

Table 1. Persistence length L_p (Å) of the cationic polymers for various chain rigidity parameters κ at different salt concentrations C_i .

κ	L_p [Å]				
	0	10	20	50	100
$C_i = 0.03$ M	39.4	44.0	48.5	55.3	59.1
$C_i = 0.01$ M	47.4	49.5	51.2	56.8	60.7
$C_i = 0.001$ M	51.7	58.5	60.1	62.6	67.7

3. Results and Discussion

3.1. Sequestration of Anionic Lipids Underneath Anchored Polymers

As an illustration of the membrane heterogeneity caused by the polymer anchoring, Figure 1 presents representative simulation snapshots of the complexes after equilibration for various chain rigidity parameters κ at two polymer concentrations. This figure clearly shows that both polymer rigidity and concentration influence the properties of the polymers/membrane complexes, which we analyze below in detail.

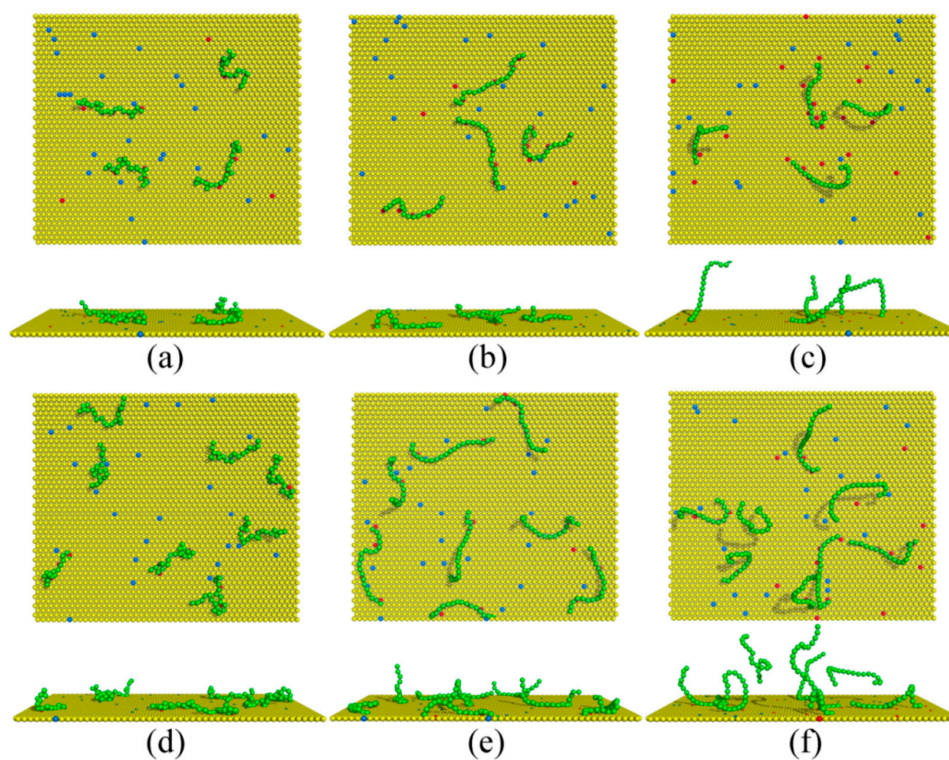


Figure 1. Equilibrated simulation snapshots of the polymers/monolayer complexes for the monolayer composition with PC:PS:PIP₂ = 98:1:1 for (a–c) $C_p = 0.00185$ and (d–f) $C_p = 0.0037$. Green spheres denote the polymer segments; yellow, blue, and red spheres represent the PC, PS, and PIP₂ lipid headgroups. The chain rigidity parameter κ of the polymers is set as (a,d) 0, (b,e) 10, and (c,f) 100, respectively.

Since each charged polymer/lipids complex minimizes its energy at the isoelectricity [1], a certain amount of anionic lipids tend to sequester around the anchored cationic polymers to achieve the charge matching. To differentiate the lipids “sequestered” by the anchored polymers from those freely diffusing on the monolayer, we use the same method as in our previous work [31,32,34], which has shown to be an efficient procedure to characterize the properties of the oppositely-charged species bounded by the charged polymers [41]. Here, we briefly introduce this method. We first define eight interaction zones on the monolayer underneath each anchored polymer. The k^{th} zone—with its size determined by the conformation of the anchored polymers in each MC step—denotes the area in a distance less than $k \times d$ (8.66 \AA) to each segment center of the anchored polymers. We then examine the system in every 50 MC steps and consider an anionic lipid “sequestered” in the k^{th} zone if it remains within the zone for this time interval. We further define the lipids sequestered in each zone as a lipid micro-domain, and calculate the number of the sequestered anionic lipids in these micro-domains. In Figure 2, we present the fraction (φ_s) of the sequestered lipids in the interaction zones of all anchored polymers, and the corresponding number (M_s) of the sequestered lipids in the zones underneath each anchored polymer for various polymer concentrations and chain rigidity parameters.

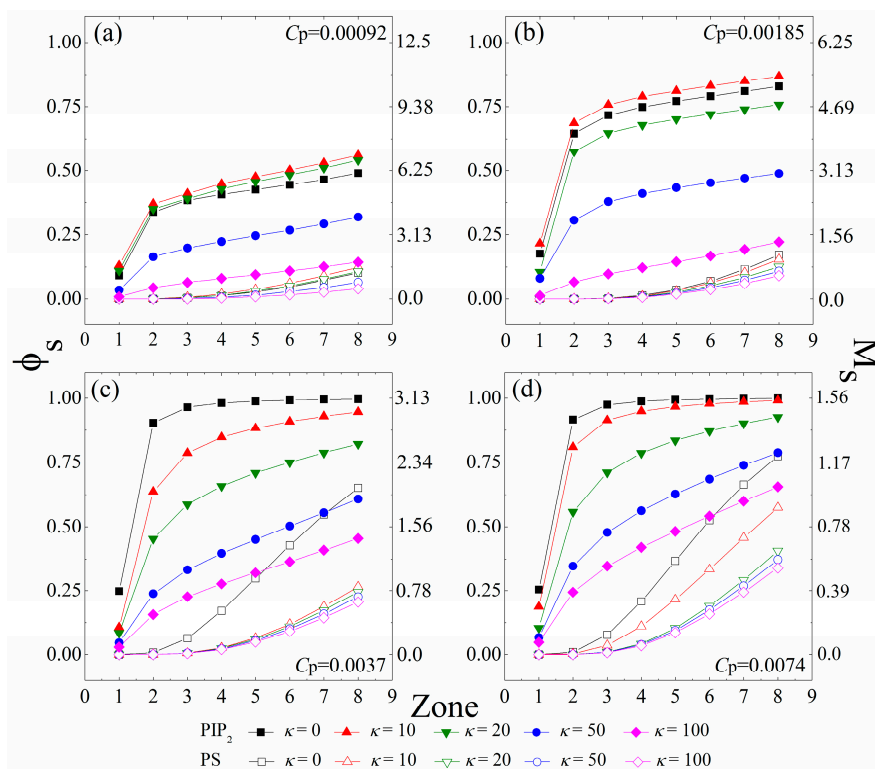


Figure 2. Fraction (ϕ_s) of the anionic lipids (PIP₂, solid symbols; PS, vacant symbols) sequestered in the interaction zones of all anchored polymers, and the number (M_s) of the anionic lipids (PIP₂, solid symbols; PS, vacant symbols) sequestered in the zones underneath each anchored polymer. The polymer concentration is set as (a) $C_p = 0.00092$; (b) $C_p = 0.00185$; (c) $C_p = 0.0037$ to (d) $C_p = 0.0074$. The chain rigidity parameter (κ) of the polymers varies from 0 to 100. The results shown are for PC:PS:PIP₂ = 98:1:1. PIP₂: phosphatidylinositol 4,5-bisphosphate; PS: Phosphatidylserine; PC: Phosphatidyl-choline.

Figure 2a,b reveal an apparent concentration gradient of the tetravalent PIP₂ lipids caused by polymer anchoring at low polymer concentrations ($C_p = 0.00092$ and 0.00185). For the cases with $\kappa = 0$ (fully flexible chains), most of the sequestered PIP₂ lipids stay in the 2nd interaction zone of the anchored polymers, whereas from the 2nd to the 8th zone, the amount of the segregated PIP₂ lipids grows slowly. Due to the lower demixing entropy loss of PIP₂ lipids for sequestration, these tetravalent lipids preferably sequester around the anchored polymers, which competitively inhibit the binding of the PS lipids. Therefore, we do not observe the PS sequestration from the 1st to the 4th zone, and only a few PS lipids randomly appear in the 5th to the 8th zones. By increasing κ from 0 (fully flexible chains, black squares) to 10 (chains with intermediate rigidity, red triangles), we find a slight growth in ϕ_s , indicating an increased amount of the PIP₂ lipids sequestered underneath the anchored polymers. However, by further increasing κ to 100 (chains with high rigidity, purple diamonds), the amount of the PIP₂ lipids sequestered in each interaction zone significantly decreases. Each polymer anchors on the monolayer when the electrostatic energy gain from neutralization exceeds the increase in the entropy loss of the system. The enhancement of chain rigidity forces the anchored polymers to flatten onto the monolayer, which contributes to the polymer anchoring through reducing its conformational entropy loss. Meanwhile, the demixing entropy loss of the anionic lipids sequestered underneath the anchored stiffer polymers is significantly enlarged, which in turn promotes dissociation of the polymers from the monolayer. This competition thus appears to rationalize our observation that the strength of interactions between the polymers and the monolayer exhibits a non-monotonic dependence on the intrinsic rigidity of polymer chains. Hence, our work reveals that the PIP₂ lipids

exhibit maximum sequestration for the anchoring of chains with intermediate rigidity ($\kappa = 10$ and 20) at low polymer concentrations.

Figure 2c,d indicate that the fraction φ_s of the total sequestered PIP₂ lipids significantly increases with increasing C_p , but each chain sequesters a lower amount of the PIP₂ lipids (indicated by a decrease in M_s) because of the inter-polymer competitions at relatively high polymer concentrations. Under these conditions, the fully flexible polymer chains can sequester nearly all PIP₂ lipids in the 3rd zones (*i.e.*, $\varphi_s \approx 1.0$) and a number of PS lipids also sequester in the 4th to 8th zones, indicating the aggregation of these univalent lipids around the polymer/PIP₂ complexes. More intriguingly, the decreased electrostatic energy gains of each polymer/PIP₂ complex cannot conquer the entropy loss of the system, because of the enhanced inter-polymer competitions for the anchoring of chains with intermediate rigidity ($\kappa = 10$ or 20). Therefore, we do not observe the non-monotonic dependence of the strength of interactions between the polymers and the monolayer on the polymer rigidity at relatively high polymer concentrations (Figure 2c,d). In these cases, the amount of the sequestered PIP₂ lipids significantly decreases with increasing κ .

Figure 3 displays the radial distribution functions (RDF) for PIP₂–PIP₂ and PS–PS lipids, which are denoted as $g_{\text{PIP}_2}(r)$ and $g_{\text{PS}}(r)$, respectively. Figure 3a,c indicate that both $g_{\text{PIP}_2}(r)$ and $g_{\text{PS}}(r)$ increase with r and gradually reach unity for the naked monolayer when polymer anchoring does not occur (purple dashed-dotted lines). When the polymer concentration is low (e.g., $C_p = 0.00092$ in Figure 3a), the flexible polymers anchor onto the monolayer and cause substantial sequestration of the PIP₂ lipids, resulting in the formation of an apparent peak in $g_{\text{PIP}_2}(r)$ at $r = 2$ ($\times 8.66 \text{ \AA}$). With κ increasing to 10 (chains with intermediate rigidity), the peak position shifts from $r = 2$ to $r = 3$ ($\times 8.66 \text{ \AA}$), and the $g_{\text{PIP}_2}(r)$ exhibits an increase at $3 < r < 8$ ($\times 8.66 \text{ \AA}$), indicating that the anchored polymers exhibit a more stretched structure and sequester a few more PIP₂ lipids in a less-compact way than the flexible ones. For chains with high rigidity (e.g., $\kappa = 50$ or 100), the polymers tend to dissociate from the monolayer, and thus fewer PIP₂ lipids are sequestered, leading to a drastic decrease in $g_{\text{PIP}_2}(r)$ at $r < 10$ ($\times 8.66 \text{ \AA}$). We also find that the corresponding $g_{\text{PS}}(r)$ at $C_p = 0.00092$ exhibits nearly the same behavior as the naked monolayer (data not shown), which illustrates that the univalent PS lipids do not sequester around the polymers in the presence of tetravalent PIP₂ lipids.

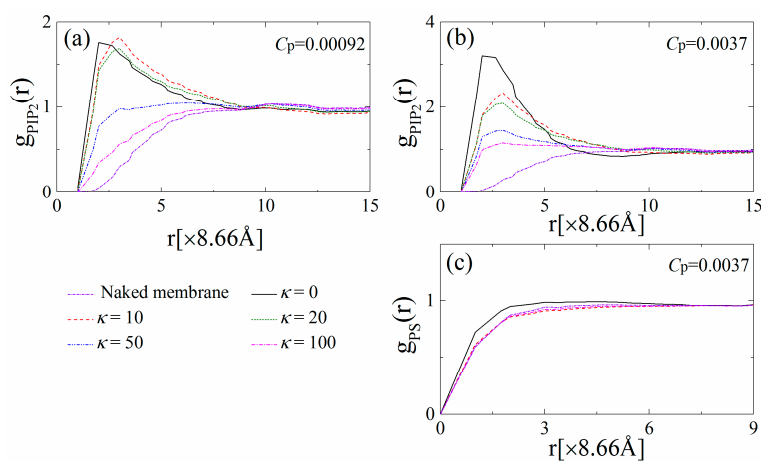


Figure 3. Radial distribution function of the PIP₂ lipids for (a) $C_p = 0.00092$ and (b) $C_p = 0.0037$ for various chain rigidity parameters κ ; (c) Radial distribution function of the PS lipids for $C_p = 0.0037$. The results shown are for PC:PS:PIP₂ = 98:1:1.

By increasing the polymer concentration to $C_p = 0.0037$, Figure 3b shows that the peak values of $g_{\text{PIP}_2}(r)$ significantly increase, indicating the increase in the total amount of the PIP₂ lipids sequestered by the concentrated anchored polymers. For the anchoring of flexible polymers, when the 1% PIP₂ lipids are not sufficient to neutralize the cationic polymers, the PS lipids accumulate around

polymer/PIP₂ complexes, and therefore $g_{PS}(r)$ at $r < 4$ ($\times 8.66$ Å) slightly increases (the solid line in Figure 3c). Further, increasing polymer chain rigidity results in the partial dissociation of the polymers and the decay of the PIP₂ sequestration, and therefore, $g_{PIP_2}(r)$ at small r significantly decreases. In addition, even if the total charge amount of the polymers exceeds those of the PIP₂ lipids, we do not observe the clustering of the PS lipids, and $g_{PS}(r)$ exhibits similar behavior as that for the naked monolayer (e.g., see the red dashed line in Figure 3c).

For comparison, we also analyze the variations of φ_s and M_s with κ and C_p for the system with PC:PIP₂ = 99:1 as well as $g_{PIP_2}(r)$ and $g_{PS}(r)$ for the systems with PC:PIP₂ = 99:1 and PC:PS:PIP₂ = 89:10:1 (data not shown). For PC:PIP₂ = 99:1, the PIP₂ sequestration exhibits a similar dependence on the rigidity and concentration of the anchored polymers as the system with PC:PS:PIP₂ = 98:1:1. For PC:PS:PIP₂ = 89:10:1, we also find the similar dependences of PIP₂ and PS redistribution on the rigidity and concentration of the anchored polymers as those for PC:PS:PIP₂ = 98:1:1. In addition, the sizable pools of the univalent PS lipids promote the polymer anchoring, which in turn enhances the sequestration of the anionic lipids, and therefore, we observe larger values of $g_{PIP_2}(r)$ for the stiffer chains compared to those for PC:PIP₂ = 99:1 and PC:PS:PIP₂ = 98:1:1.

3.2. Distribution of the Anchored Polymer Segments

We now focus on the properties of the anchored polymers in order to further elucidate the interactions between the polymers and the anionic lipids. In particular, we examine the distribution function $g_s(r)$ for the segments of the anchored polymers above the monolayer surface. Figure 4a indicates a shoulder peak in $g_p(r)$ for the fully flexible chains when the polymer concentration is low (i.e., $C_p = 0.00092$), which is due to the presence of segments in the loops and tails of the anchored polymers. The observation of a shoulder peak in $g_p(r)$ corresponds well with the previous simulation results for the adsorption of charged polymers on oppositely-charged interfaces [42]. Moreover, the chains with intermediate rigidity ($\kappa = 10$) flatten onto the monolayer, resulting in a slight increase in the contact value of $g_p(r)$ at $r < 1$ ($\times 8.66$ Å), but the decay of the shoulder peak at $1 < r < 2$ ($\times 8.66$ Å). This result implies that the increased cooperative effects between the anchored cationic segments can enhance the sequestration and restriction of the anionic lipids. By further increasing κ from 20 to 100, the anchored polymers tend to dissociate from the monolayer, which leads to an apparent decrease in the peak values of $g_p(r)$ and an increase in $g_p(r)$ at $r > 2$ ($\times 8.66$ Å). In Figure 4b, we show the results of $g_p(r)$ for $C_p = 0.0037$. The polymers contend for anchoring onto the monolayer at this concentration, and therefore, we observe an apparent decrease in the contact value of $g_p(r)$ compared to the results in Figure 4a. The enhancement of the polymer chain rigidity results in the partial dissociation of the anchored polymers, and hence, the contact value of $g_p(r)$ decreases with increasing κ —indicating that the polymers exhibit the brush-like conformations. This analysis supports our earlier observation that the partially dissociated stiffer polymers sequester smaller lipid clusters at relatively high polymer concentrations.

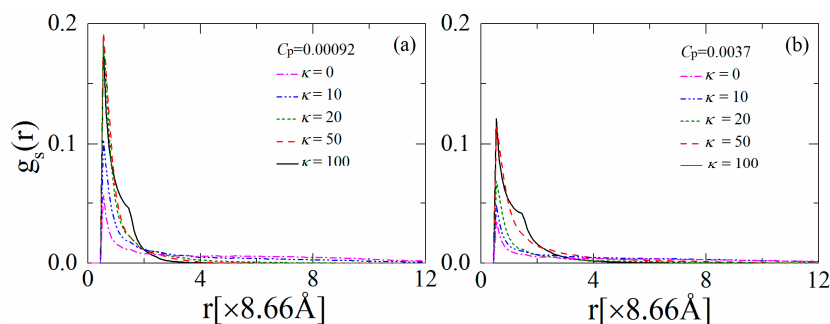


Figure 4. Distribution function for segments of the anchored polymers on the monolayer for various polymer chain rigidity parameters κ for (a) $C_p = 0.00092$ and (b) $C_p = 0.0037$. The results shown are for PC:PS:PIP₂ = 98:1:1.

3.3. Restricted Mobility of the Polymer/Lipids Complexes

Prior experimental studies have demonstrated that the anchored cationic polymers can significantly slow down the mobility of the sequestered lipids, which in turn exerts a restriction on the dynamics of the anchored polymers [9,23]. To qualitatively capture the mobility of the polymers/monolayer complexes, we calculate the mean-square-displacement (MSD) of each lipid micro-domain as well as the single sequestered lipids in it in every 50 MC steps, denoted as m_d and m_l , respectively. We also analyze the corresponding MSD of the center of mass of the anchored polymers, denoted as m_{pc} . Our previous simulation results [31,32] show that the cationic polymer can cause significant sequestration of the anionic lipids and thus reduce their translational mobility, which is in qualitative agreement with recent experimental measurements [7]. Moreover, we illustrate that the mobility of a flexible cationic polymer anchored on the monolayer satisfies the scaling of $m_p \sim N^{-1}$ (where N is the polymerization degree of polymers). This scaling was also observed in a previous experimental study [43]. This implies that our simulations may provide a reliable tool for understanding the mobility of polymers/lipids complexes in the equilibrium state, at least in a qualitative manner despite the rather idealized nature of our model. We now discuss the effects of the rigidity and concentration of the anchored polymers on the restricted mobility of the polymers/monolayer complexes.

Figure 5 shows m_{pc} as a function of the chain rigidity parameter κ for various polymer concentrations C_p . Our earlier analysis indicates that the polymers/monolayer interactions are strengthened with increasing κ from 0 to 10 when the polymer concentration is low. As a consequence, we find that m_{pc} first slightly decreases with increasing chain rigidity for low polymer concentrations, indicating a slower mobility of the anchored polymers. By further increasing κ from 20 to 100, the cationic polymers tend to dissociate from the monolayer and protrude longer tails into the solution, and thus exhibit a faster mobility, as evidenced by a significant increase in m_{pc} . The variation of m_{pc} with κ changes both quantitatively and qualitatively when the polymer concentration is high. In this case, the inter-chain competitions promote the dissociation of each polymer from the monolayer; therefore, we observe a significant increase in m_{pc} as compared to the results at low polymer concentrations. In addition, the interactions between the monolayer and the polymers are significantly weakened with increasing the chain rigidity at high polymer concentrations, where the mobility of the anchored polymers monotonically increases with increasing the chain rigidity.

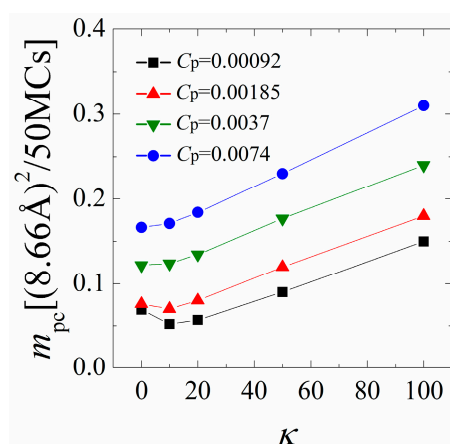


Figure 5. Mean-square-displacement (MSD) of the center of mass of the anchored polymers calculated in every 50 Monte Carlo (MC) steps as a function of chain rigidity parameter κ for various polymer concentrations. The results shown are for PC:PS:PIP₂ = 98:1:1.

We now investigate the mobility of the sequestered anionic lipid clusters underneath the anchored cationic polymers. Figure 6a indicates that the mobility of lipid clusters enhances from the 2nd to the

8th zone at low polymer concentrations ($C_p = 0.00092$), a trend that arises because the electrostatic attractions from the anchored cationic polymers weaken from the 2nd to the 8th zone at such concentrations. The PIP₂ lipids sequestered by anchored polymers with $\kappa = 10$ become more restricted than by flexible polymers ($\kappa = 0$), as evidenced by a corresponding decrease in m_{d-PIP_2} . By increasing κ from 20 to 100, we observe that the PIP₂ clusters also exhibit a faster mobility. This result accords well with previous MC simulation work [23], which has shown that the electrostatically-bound anionic PIP₂ clusters migrate with the cationic polymers together. Recent experiments have shown the trapping of PIP₂ lipids by peripheral cationic polymers and emphasized the mobility coupling between polymers and PIP₂ lipids [7,9]. Our simulations are also in good agreement with these experimental results. Figure 6b indicates that increasing the polymer concentration to $C_p = 0.00185$ leads to a decrease in the mobility of the sequestered PIP₂ lipid cluster. The increase in C_p enhances the competition between the anchored polymers, resulting in the formation of the smaller sequestered PIP₂ lipid clusters. These smaller clusters can only move in the smaller interaction zones underneath the partially adsorbed polymers, and their mobility is more confined—as evidenced by a decrease in m_{d-PIP_2} . Due to the enhanced competitions between anchored polymers, the chains with $\kappa = 20$ exert weaker attractions on the monolayer than the flexible ones for $C_p = 0.00185$, which results in the formation of smaller PIP₂ clusters with a decreased mobility.

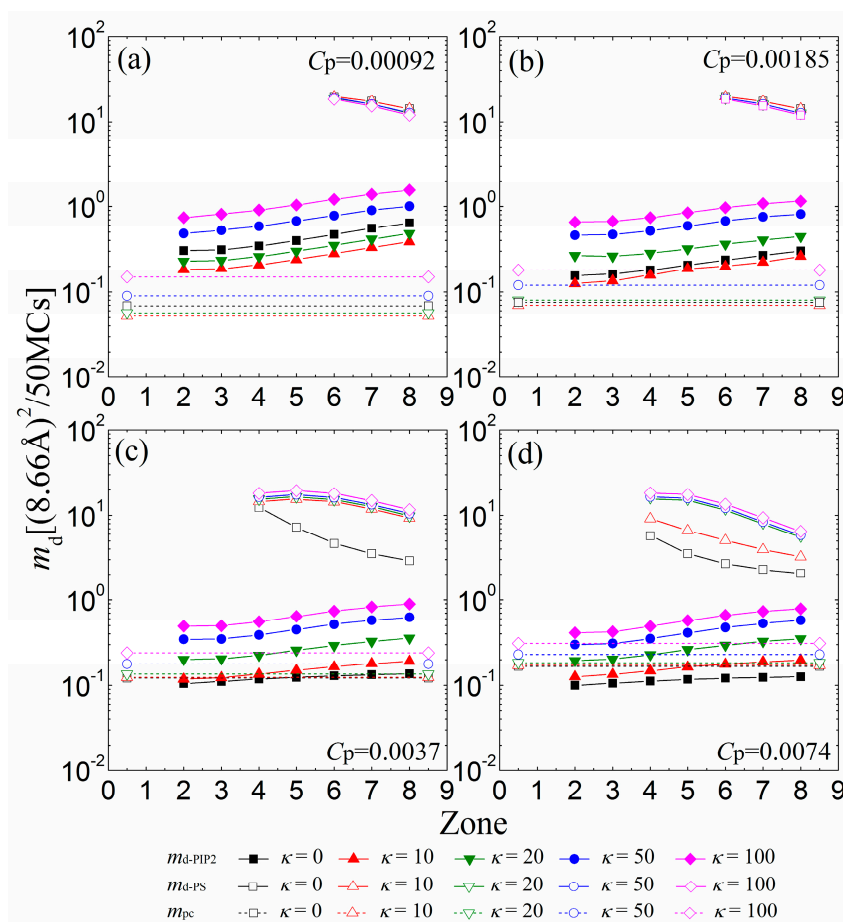


Figure 6. MSD of the center of mass of the sequestered PIP₂ micro-domains (m_{d-PIP_2} , solid symbols and solid lines) and PS micro-domains (m_{d-PS} , vacant symbols and solid lines) calculated in every 50 MC steps for various chain rigidity parameters κ for (a) $C_p = 0.00092$; (b) $C_p = 0.00185$; (c) $C_p = 0.0037$; and (d) $C_p = 0.0074$. Vacant symbols with dashed lines indicate m_{pc} of the anchored polymers. The results shown are for PC:PS:PIP₂ = 98:1:1.

For $C_p = 0.0037$ (Figure 6c) and $C_p = 0.0074$ (Figure 6d), the competitions among the anchored polymers are significantly strengthened, which leads to the further shrinkage of the sequestered PIP₂ lipid clusters underneath fewer anchored segments of each polymer. These small lipid clusters are firmly restricted by the reduced anchored segments of the polymers, and therefore, we observe a decrease in the mobility of each PIP₂ cluster compared with the cases for lower polymer concentrations. Importantly, the polymers with intermediate rigidity no longer exert stronger adsorption on the monolayer than the flexible ones because of the inter-polymer competitions; hence, the mobility of the PIP₂ clusters exhibits a monotonic dependence on the polymer chain rigidity. For sufficiently high polymer concentrations, only the polymers with small rigidity parameters (e.g., $C_p = 0.0037$ and $\kappa = 0$ in Figure 6c; $C_p = 0.0074$ and $\kappa \leq 10$ in Figure 6d) can overcharge the PIP₂ lipids and further restrict the PS lipids (see the vacant squares and triangles with solid lines in Figure 6c,d), whereas the stiffer polymer chains cannot firmly adsorb on the monolayer and barely affect the mobility of the PS lipids. Our results imply that the polymers with high rigidity can serve to sequester and differentiate the multivalent lipids from the univalent ones through the electrostatic anchoring at sufficiently high polymer concentrations.

3.4. Mobility Gradient in Lipid Clusters

To analyze the mobility gradient of the anionic lipids within each sequestered lipid cluster, Figure 7 displays the MSD of single PIP₂ (m_{1-PIP_2}) and PS (m_{1-PS}) lipids confined in the interaction zones underneath the anchored polymers. For the polymer concentration of $C_p = 0.00092$ shown in Figure 7a, the connected anchored segments of each polymer form several interaction zones, where the sequestered lipids can freely hop on different sites with the similar electrostatic fields. At this polymer concentration, chains with intermediate rigidity ($\kappa = 10$ or 20) tend to flatten onto the monolayer. The increased anchored segments of these chains create larger electrostatic homogeneous interaction zones on the monolayer. Therefore, the single PIP₂ lipids restricted in the larger 1st or 2nd zones of these chains can freely hop on any site in these larger 1st or 2nd zones, and exhibit a faster mobility (e.g., filled red triangles in Figure 7a) than the ones confined within the smaller 1st or 2nd zones created by the lessened anchored segments of the flexible polymers (filled black squares in Figure 7a). In addition, the stronger cooperative effects between the increased cationic segments are enhanced in the larger zones (e.g., the 6th to the 8th) of the polymers with these intermediate rigidities. The PIP₂ lipids confined in these larger zones (e.g., the 6th to the 8th) encounter stronger restrictions from the increased anchored cationic segments of the flattened polymers with intermediate rigidity, and exhibit a slower mobility (e.g., filled red triangles in Figure 7a) than those confined in the corresponding zones of flexible polymers (e.g., filled black squares in Figure 7a). Due to the decay in the cooperative effects between the lessened anchored segments, the PIP₂ lipids sequestered in the 1st or 2nd zones suffer stronger restrictions and exhibit a slower mobility for the polymers with high rigidity ($\kappa \geq 50$), whereas those sequestered in larger zones display a faster mobility, indicating a sharper mobility gradient of the PIP₂ clusters. By increasing the polymer concentration to $C_p = 0.00185$ (Figure 7b), we observe that the mobility of single PIP₂ lipids exhibits a similar dependence as the case for $C_p = 0.00092$ (Figure 7a). The enhanced competitions between anchored polymers ($C_p = 0.00185$) causes the reduced anchored segments for $\kappa = 20$ to exhibit weaker cooperative effects than those for $\kappa = 0$. Therefore, the PIP₂ lipids sequestered in the 1st or 2nd zones exhibit a slower mobility, while those sequestered in larger zones display a faster mobility.

For higher polymer concentrations (e.g., $C_p = 0.0037$ and $C_p = 0.0074$, shown in Figure 7c,d), the polymers sequester nearly all PIP₂ lipids. Meanwhile, the anchored polymers tend to exhibit a brush-like structure because of the enhanced inter-chain competitions, which greatly diminishes the cooperative effects between anchored segments. In each polymer/PIP₂ complex, the fewer anchored segments exert stronger restrictions on the lessened PIP₂ lipids; therefore, the mobility of the PIP₂ lipids confined in each zone presents a decrease compared to the case for low polymer concentrations. The cooperative effects between the lessened anchored segments weaken with increasing chain rigidity,

which results in the sharper mobility gradient of the sequestered PIP₂ lipids. In addition, we only find a significant decrease in m_{1-PS} for $\kappa = 0$ at $C_p = 0.0037$ and $\kappa \leq 10$ at $C_p = 0.0074$. This also demonstrates that the PS lipids can only sequester around the anchored flexible polymers, even if the total charge amount of the polymers is larger than that of the PIP₂ lipids.

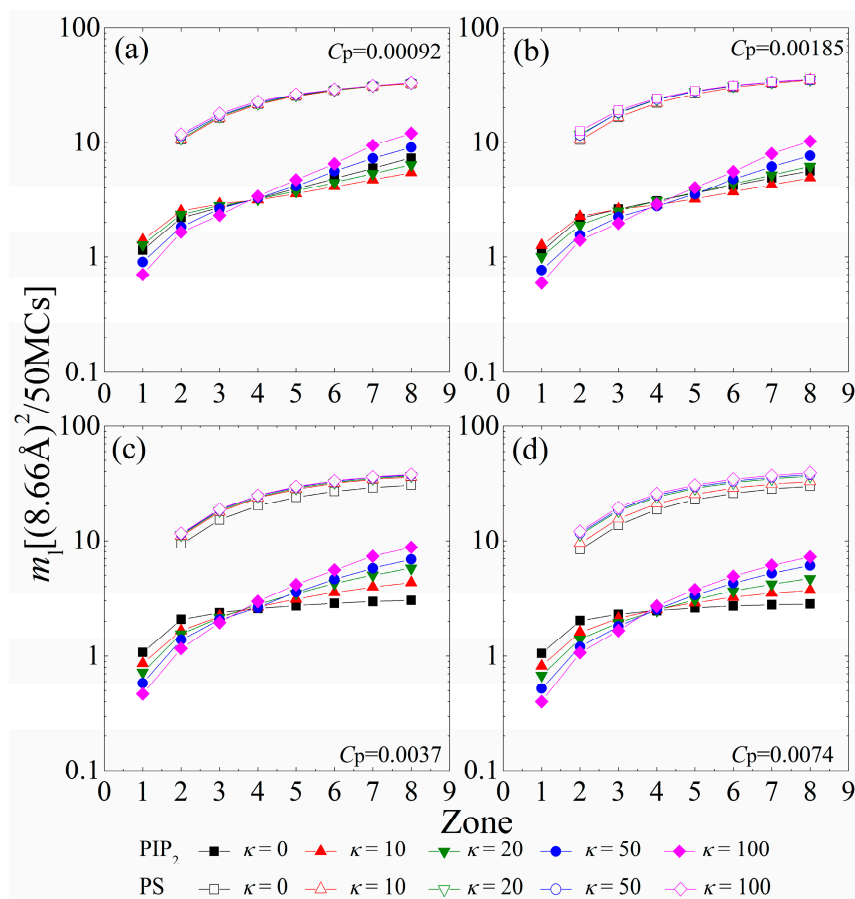


Figure 7. MSD of single PIP₂ (m_{1-PIP_2} , solid symbols and solid lines) and single PS (m_{1-PS} , vacant symbols and solid lines) sequestered in each interaction zone calculated in every 50 MC steps for various chain rigidity parameters κ for (a) $C_p = 0.00092$; (b) $C_p = 0.00185$; (c) $C_p = 0.0037$; and (d) $C_p = 0.0074$. The results shown are for PC:PS:PIP₂ = 98:1:1.

Our results thus illustrate the complicated mobility behavior of the polymers/lipids complexes. The sequestered anionic lipids exhibit hierarchical mobility, which is sensitively modulated by the chain rigidity and concentration of the cationic polymers. We also analyze the effects of rigidity and concentration of the anchored polymers on the restricted mobility of the polymers/monolayer complexes with the monolayer compositions of PC:PIP₂ = 99:1 and PC:PS:PIP₂ = 89:10:1. For both cases, we also find similar dependences of m_{PC} , m_d , and m_1 on the rigidity and concentration of the anchored polymers (data not shown). The simulation results for PC:PS:PIP₂ = 89:10:1 appear to serve as a rationale for the formation of membrane heterogeneity with realistic lipid compositions. Due to the enhanced electrostatic interactions between the cationic polymers and the monolayer, m_{PC} , m_d , and m_1 slightly decrease compared with the results for PC:PS:PIP₂ = 98:1:1. Finally, we explore the salt effect of the solution on the polymers/monolayer interactions, and we find that the screening effect of the solution with higher salt concentrations can drastically weaken the polymer anchoring and lipid sequestration. Under this condition, the anchored polymers, lipid clusters, and single sequestered lipids exhibit faster motilities. Our results are thus consistent with previous experiments showing that the extent of the PIP₂ sequestration decreases as the salt concentration increases [8].

4. Conclusions

In this work, we have explored the interactions between anchored cationic polymers and a mixed fluid lipid monolayer composed of charge-neutral, univalent, and tetravalent anionic lipids using Monte Carlo simulations. In particular, we systematically examine the effects of the chain rigidity and concentration of polymers on the spatial sequestration and mobility heterogeneity of different anionic lipids. Our simulation results illustrate that the tetravalent anionic PIP₂ lipids preferentially sequester around the anchored cationic polymers, and migrate with polymers together on the monolayer. Increasing the polymer chain intrinsic rigidity enlarges the demixing entropy loss of the sequestered anionic lipids but diminishes the conformational entropy loss of the anchored cationic polymers. Due to this energy–entropy competition, the polymers/monolayer interaction strength exhibits a non-monotonic dependence on the chain rigidity at low polymer concentrations. Polymers with intermediate rigidity exhibit the maximal anchoring ability on the monolayer, which results in the formation of larger sequestered PIP₂ clusters and slower mobility of the polymer/PIP₂ complexes. On the other hand, the enhanced inter-polymer competitions result in reduced electrostatic energy gains for each polymer/lipids complex at sufficiently high polymer concentrations. Under such conditions, the polymers/monolayer interaction strength monotonically decreases with increasing chain rigidity. The anchored flexible polymers can confine nearly all the tetravalent PIP₂ lipids and further sequester the univalent PS lipids around the polymer/PIP₂ complexes, whereas the stiffer polymers tend to partially dissociate from the monolayer and only sequester smaller PIP₂ clusters with an increased mobility. We further illustrate that the mobility gradient of the single PIP₂ lipids is sensitively modulated by the cooperative effects between anchored segments of the polymers in the sequestered lipid clusters. Therefore, our work demonstrates that the structural and dynamical properties of the anionic lipids can be regulated by adjusting the rigidity and concentration of the anchored polymers.

Acknowledgments: This work is supported by the National Natural Science Foundation of China (No. 21234007, 21404103 and 51473168) and the Special Program for Applied Research on Super Computation of the NSFC-Guangdong Joint Fund (the second phase). We are grateful to the Computing Center of Jilin Province for essential support.

Author Contributions: Xiaozheng Duan, Ran Zhang, Mingming Ding, Tongfei Shi, Qingrong Huang, Lijia An and Wen-Sheng Xu conceived and designed the simulations; Xiaozheng Duan, Yang Zhang, Mingming Ding and Wen-Sheng Xu performed the simulations; Xiaozheng Duan, Mingming Ding and Wen-Sheng Xu analyzed the data; Xiaozheng Duan, Yang Zhang, Mingming Ding, Tongfei Shi and Wen-Sheng Xu interpreted the results and wrote the paper.

Conflicts of Interest: The authors declare no conflicts of interest. The founding sponsors had no role in the design of the study; in the collection, analyses, or interpretation of data; in the writing of the manuscript, and in the decision to publish the results.

Abbreviations

The following abbreviations are used in this manuscript:

PC	Phosphatidyl-choline
PS	Phosphatidylserine
PIP ₂	Phosphatidylinositol 4,5-bisphosphate
MC	Monte Carlo
MSD	Mean-square-displacement
RDF	Radial distribution function
BAC	Bond angle correlation function
L_p	Persistence length
l_B	Bjerrum length
l_D^-	Debye screening length
κ	Parameter to tailor the degree of polymer chain rigidity
C_p	Polymer concentration
φ_s	Fraction of the sequestered lipids in the interaction zones of all anchored polymers
M_s	Number of the sequestered lipids in the zones underneath each anchored polymer

$g_{PIP_2}(r)$	Radial distribution function for PIP ₂ –PIP ₂ lipids
$g_{PS}(r)$	Radial distribution function for PS–PS lipids
$g_s(r)$	Distribution of the segments of the anchored polymers above the monolayer surface
m_{pc}	MSD of the center of mass of the anchored polymers
m_{pd}	MSD of lipid micro-domain
m_{pl}	MSD of single sequestered lipids

References

- McLaughlin, S.; Murray, D. Plasma membrane phosphoinositide organization by protein electrostatics. *Nature* **2005**, *438*, 605–611. [[CrossRef](#)] [[PubMed](#)]
- Vance, J.E.; Steenbergen, R. Metabolism and functions of phosphatidylserine. *Prog. Lipid Res.* **2005**, *44*, 207–234. [[CrossRef](#)] [[PubMed](#)]
- McLaughlin, S.; Wang, J.Y.; Gambhir, A.; Murray, D. PIP₂ AND proteins: Interactions, organization, and information flow. *Annu. Rev. Biophys. Biomol.* **2002**, *31*, 151–175. [[CrossRef](#)] [[PubMed](#)]
- Di Paolo, G.; De Camilli, P. Phosphoinositides in cell regulation and membrane dynamics. *Nature* **2006**, *443*, 651–657. [[CrossRef](#)] [[PubMed](#)]
- Heo, W.D.; Inoue, T.; Park, W.S.; Kim, M.L.; Park, B.O.; Wandless, T.J.; Meyer, T. PI(3,4,5)P-3 and PI(4,5)P-2 lipids target proteins with polybasic clusters to the plasma membrane. *Science* **2006**, *314*, 1458–1461. [[CrossRef](#)] [[PubMed](#)]
- Yeung, T.; Gilbert, G.E.; Shi, J.; Silvius, J.; Kapus, A.; Grinstein, S. Membrane phosphatidylserine regulates surface charge and protein localization. *Science* **2008**, *319*, 210–213. [[CrossRef](#)] [[PubMed](#)]
- Shi, X.J.; Li, X.S.; Kaliszewski, M.J.; Zhuang, X.D.; Smith, A.W. Tuning the mobility coupling of quaternized polyvinylpyridine and anionic phospholipids in supported lipid bilayers. *Langmuir* **2015**, *31*, 1784–1791. [[CrossRef](#)] [[PubMed](#)]
- Gambhir, A.; Hangyas-Mihalyne, G.; Zaitseva, I.; Cafiso, D.S.; Wang, J.Y.; Murray, D.; Pentylala, S.N.; Smith, S.O.; McLaughlin, S. Electrostatic sequestration of PIP₂ on phospholipid membranes by basic/aromatic regions of proteins. *Biophys. J.* **2004**, *86*, 2188–2207. [[CrossRef](#)]
- Golebiewska, U.; Gambhir, A.; Hangyas-Mihalyne, G.; Zaitseva, I.; Radler, J.; McLaughlin, S. Membrane-bound basic peptides sequester multivalent (PIP₂), but not monovalent (PS), acidic lipids. *Biophys. J.* **2006**, *91*, 588–599. [[CrossRef](#)] [[PubMed](#)]
- Shi, X.J.; Kohram, M.; Zhuang, X.D.; Smith, A.W. Interactions and translational dynamics of phosphatidylinositol bisphosphate (PIP₂) lipids in asymmetric lipid bilayers. *Langmuir* **2016**, *32*, 1732–1741. [[CrossRef](#)] [[PubMed](#)]
- Cai, X.M.; Lietha, D.; Ceccarelli, D.F.; Karginov, A.V.; Rajfur, Z.; Jacobson, K.; Hahn, K.M.; Eck, M.J.; Schaller, M.D. Spatial and temporal regulation of focal adhesion kinase activity in living cells. *Mol. Cell. Biol.* **2008**, *28*, 201–214. [[CrossRef](#)] [[PubMed](#)]
- Sarkar, J.; Annepu, H.; Sharma, A. Contact instability of a soft elastic film bonded to a patterned substrate. *J. Adhesion* **2011**, *87*, 214–234. [[CrossRef](#)]
- Yan, H.D.; Villalobos, C.; Andrade, R. TRPC channels mediate a muscarinic receptor-induced afterdepolarization in cerebral cortex. *J. Neurosci.* **2009**, *29*, 10038–10046. [[CrossRef](#)] [[PubMed](#)]
- Yeh, L.H.; Xue, S.; Joo, S.W.; Qian, S.; Hsu, J.P. Field effect control of surface charge property and electroosmotic flow in nanofluidics. *J. Phys. Chem. C* **2012**, *116*, 4209–4216. [[CrossRef](#)]
- Mollapour, M.; Phelan, J.P.; Millson, S.H.; Piper, P.W.; Cooke, F.T. Weak acid and alkali stress regulate phosphatidylinositol bisphosphate synthesis in *Saccharomyces cerevisiae*. *Biochem. J.* **2006**, *395*, 73–80. [[CrossRef](#)] [[PubMed](#)]
- Im, Y.J.; Perera, I.Y.; Brglez, I.; Davis, A.J.; Stevenson-Paulik, J.; Phillippy, B.Q.; Johannes, E.; Allen, N.S.; Boss, W.F. Increasing plasma membrane phosphatidylinositol(4,5)bisphosphate biosynthesis increases phosphoinositide metabolism in *Nicotiana tabacum*. *Plant Cell* **2007**, *19*, 1603–1616. [[CrossRef](#)] [[PubMed](#)]
- McLaughlin, S. The electrostatic properties of membranes. *Ann. Rev. Biophys. Biophys. Chem.* **1989**, *18*, 113–136. [[CrossRef](#)] [[PubMed](#)]
- Haleva, E.; Ben-Tal, N.; Diamant, H. Increased PIP₂ concentration of polyvalent phospholipids in the adsorption domain of a charged protein. *Biophys. J.* **2004**, *86*, 2165–2178. [[CrossRef](#)]

19. Mbamala, E.C.; Ben-Shaul, A.; May, S. Domain formation induced by the adsorption of charged proteins on mixed lipid membranes. *Biophys. J.* **2005**, *88*, 1702–1714. [[CrossRef](#)] [[PubMed](#)]
20. Dias, R.S.; Pais, A.; Linse, P.; Miguel, M.G.; Lindman, B. Polyion adsorption onto catanionic surfaces. A Monte Carlo study. *J. Phys. Chem. B* **2005**, *109*, 11781–11788. [[CrossRef](#)] [[PubMed](#)]
21. Loew, S.; Hinderliter, A.; May, S. Stability of protein-decorated mixed lipid membranes: The interplay of lipid-lipid, lipid-protein, and protein-protein interactions. *J. Chem. Phys.* **2009**, *130*, 045102. [[CrossRef](#)] [[PubMed](#)]
22. Tzlil, S.; Ben-Shaul, A. Flexible charged macromolecules on mixed fluid lipid membranes: Theory and Monte Carlo simulations. *Biophys. J.* **2005**, *89*, 2972–2987. [[CrossRef](#)] [[PubMed](#)]
23. Khelashvili, G.; Weinstein, H.; Harries, D. Protein diffusion on charged membranes: A dynamic mean-field model describes time evolution and lipid reorganization. *Biophys. J.* **2008**, *94*, 2580–2597. [[CrossRef](#)] [[PubMed](#)]
24. Tzlil, S.; Murray, D.; Ben-Shaul, A. The “Electrostatic-Switch” mechanism: Monte Carlo study of MARCKS-membrane interaction. *Biophys. J.* **2008**, *95*, 1745–1757. [[CrossRef](#)] [[PubMed](#)]
25. Kiselev, V.Y.; Marenduzzo, D.; Goryachev, A.B. Lateral dynamics of proteins with polybasic domain on anionic membranes: A dynamic Monte-Carlo study. *Biophys. J.* **2011**, *100*, 1261–1270. [[CrossRef](#)] [[PubMed](#)]
26. Tian, W.D.; Ma, Y.Q. Theoretical and computational studies of dendrimers as delivery vectors. *Chem. Soc. Rev.* **2013**, *42*, 705–727. [[CrossRef](#)] [[PubMed](#)]
27. Tu, C.K.; Chen, K.; Tian, W.D.; Ma, Y.Q. Computational investigations of a peptide-modified dendrimer interacting with lipid membranes. *Macromol. Rapid Commun.* **2013**, *34*, 1237–1242. [[CrossRef](#)] [[PubMed](#)]
28. Bradley, R.; Radhakrishnan, R. Coarse-Grained models for protein-cell membrane interactions. *Polymers* **2013**, *5*, 890–936. [[CrossRef](#)] [[PubMed](#)]
29. Liu, Y.C.; Storm, D.R. Regulation of free calmodulin levels by neuromodulin—Neuron growth and regeneration. *Trends Pharmacol. Sci.* **1990**, *11*, 107–111. [[PubMed](#)]
30. Duan, X.Z.; Zhang, R.; Li, Y.Q.; Shi, T.F.; An, L.J.; Huang, Q.R. Monte Carlo study of polyelectrolyte adsorption on mixed lipid membrane. *J. Phys. Chem. B* **2013**, *117*, 989–1002. [[CrossRef](#)] [[PubMed](#)]
31. Duan, X.Z.; Li, Y.Q.; Zhang, R.; Shi, T.F.; An, L.J.; Huang, Q.R. Regulation of anionic lipids in binary membrane upon the adsorption of polyelectrolyte: A Monte Carlo simulation. *AIP Adv.* **2013**, *3*, 062128. [[CrossRef](#)]
32. Duan, X.Z.; Zhang, R.; Li, Y.Q.; Yang, Y.B.; Shi, T.F.; An, L.J.; Huang, Q.R. Effect of polyelectrolyte adsorption on lateral distribution and dynamics of anionic lipids: A Monte Carlo study of a coarse-grain model. *Eur. Biophys. J.* **2014**, *43*, 377–391. [[CrossRef](#)] [[PubMed](#)]
33. Duan, X.Z.; Ding, M.M.; Zhang, R.; Li, L.Y.; Shi, T.F.; An, L.J.; Huang, Q.R.; Xu, W.S. Effects of chain rigidity on the adsorption of a polyelectrolyte chain on mixed lipid monolayer: A Monte Carlo study. *J. Phys. Chem. B* **2015**, *119*, 6041–6049. [[CrossRef](#)] [[PubMed](#)]
34. Duan, X.Z.; Li, Y.Q.; Zhang, R.; Shi, T.F.; An, L.J.; Huang, Q.R. Compositional redistribution and dynamic heterogeneity in mixed lipid membrane induced by polyelectrolyte adsorption: Effects of chain rigidity. *Eur. Phys. J. E* **2014**, *37*, 71. [[CrossRef](#)] [[PubMed](#)]
35. Wang, L.; Liang, H.J.; Wu, J.Z. Electrostatic origins of polyelectrolyte adsorption: Theory and Monte Carlo simulations. *J. Chem. Phys.* **2010**, *133*, 044906. [[CrossRef](#)] [[PubMed](#)]
36. Zhang, R.; Duan, X.Z.; Shi, T.F.; Li, H.F.; An, L.J.; Huang, Q.R. Physical gelation of polypeptide-polyelectrolyte-polypeptide (ABA) copolymer in solution. *Macromolecules* **2012**, *45*, 6201–6209. [[CrossRef](#)]
37. Kawasaki, K. *Phase Transition and Critical Phenomena*; Domb, C., Green, M.S., Eds.; Academic Press: New York, NY, USA, 1972; Volume 2.
38. Jan, N.; Lookman, T.; Pink, D.A. On computer-simulation methods used to study models of 2-component lipid bilayers. *Biochemistry* **1984**, *23*, 3227–3231. [[CrossRef](#)] [[PubMed](#)]
39. Metropolis, N.; Rosenbluth, A.W.; Rosenbluth, M.N.; Teller, A.H.; Teller, E. Equation of state calculations by fast computing machines. *J. Chem. Phys.* **1953**, *21*, 1087–1092. [[CrossRef](#)]
40. Stoll, S.; Chodanowski, P. Polyelectrolyte adsorption on an oppositely charged spherical particle. Chain rigidity effects. *Macromolecules* **2002**, *35*, 9556–9562. [[CrossRef](#)]
41. Liu, S.; Muthukumar, M. Langevin dynamics simulation of counterion distribution around isolated flexible polyelectrolyte chains. *J. Chem. Phys.* **2002**, *116*, 9975–9982. [[CrossRef](#)]

42. Akesson, T.; Woodward, C.; Jonsson, B. Electric double-layer forces in the presence of poly-electrolytes. *J. Chem. Phys.* **1989**, *91*, 2461–2469. [[CrossRef](#)]
43. Maier, B.; Radler, J.O. Conformation and self-diffusion of single DNA molecules confined to two dimensions. *Phys. Rev. Lett.* **1999**, *82*, 1911–1914. [[CrossRef](#)]



© 2016 by the authors; licensee MDPI, Basel, Switzerland. This article is an open access article distributed under the terms and conditions of the Creative Commons Attribution (CC-BY) license (<http://creativecommons.org/licenses/by/4.0/>).